ELSEVIER

Journal of Nuclear Materials 245 (1997) 115–123

journal of nuclear materials

An electron microscopy study of the RIM structure of a UO_2 fuel with a high burnup of 7.9% FIMA

I.L.F. Ray [a], Hj. Matzke [a,*], H.A. Thiele [a], M. Kinoshita [b]

[a] *European Commission, Joint Research Centre, Institute for Transuranium Elements, Postfach 2340, D-76125 Karlsruhe, Germany*
[b] *Central Research Institute of Electric Power Industry (CRIEPI), 2-11-1 Iwadokita, Komaeshi, Tokyo, Japan*

Received 23 September 1996; accepted 24 February 1997

Abstract

Transmission and high resolution scanning electron microscopy were used to analyze the microstructure of the periphery of a UO_2 pellet irradiated to a cross-section average burnup of 7.9% FIMA, with a period of increased temperature at about half the final burnup. Local burnups at the pellet surface reached nearly 23% FIMA. In this rim region the original grains of about 10 μm diameter were subdivided into about 10^4 subgrains of 0.15 to 0.30 μm diameter. The spread in subgrain orientation was small ($< 5°$). The typical small fission gas bubbles present in the cold part of UO_2 irradiated to lower burnups of $\simeq 40$ GWd/tM were not found in this zone. The center of the same cross-section showed no grain subdivision. Rather, the typical dislocations, dislocation loops, gas bubbles and five-metal particles were found. The high burnup structure extended to a depth of 1.65 mm. The proportions of grains showing this structure decreased from 100% at the fuel surface to very small values at depths > 1 mm. The size of the subgrains was found to be largely independent of depth.

1. Introduction

The peripheral region (the 'rim') of high burnup UO_2 fuel develops a particular microstructure known as the 'rim structure' [1–3], the appearance of which was previously described as a 'cauliflower-structure' [1]. In earlier work, it was stated to be characterized by 'a loss of observable grain structure', a statement which was later modified to 'a loss of optically-definable grain structure'. There is a marked decrease in the apparent grain size, accompanied by an increase in porosity and a decrease in the signal for fission xenon as measured by electron probe microanalysis, EPMA. These microstructural changes first occur when the average burnup exceeds about 40 GWd/tM. At fuel cross-section-averaged burnups below $\simeq 60$ GWd/tM, this structure is confined to a width of about 150 to 200 μm, hence to the peripheral or rim region. In this region, the local burnup is higher by a factor of up to $\simeq 2.5$ due to neutron resonance capture of U-238 causing a locally increased concentration of fissile Pu-239 (e.g. [2]). The mechanism leading to the formation of this rim microstructure (grain subdivision or polygonization) is not fully satisfactorily understood at the present time.

Transmission electron microscopy (TEM) and scanning electron microscopy (SEM) have been used to make a detailed analysis of the microstructure of samples taken from the periphery of a UO_2 pellet irradiated to an average burnup of 7.9% FIMA (74 GWd/tM), but with a local burnup at the pellet surface of up to 23% FIMA. The question of whether and how much this grain subdivision process can extend into the interior of the fuel is of great interest. The fact that it is not restricted to this shallow rim zone at high burnup has been known for some years. In the present work, the investigation of the fuel structure was continued with a SEM examination of large residual pieces of the above fuel, extending the radial depth of the investigation to nearly 2 mm. The specific fuel used was selected since it experienced a period of increased rating and hence high temperatures and increased local gas release at about half its burnup. It is thought that this helps to understand the parameters (burnup, temperature, fission gas content, damage configuration) important for polygonization of LWR fuel.

* Corresponding author. Tel.: +49-7247 951 273; fax: +49-7247 951 590.

PII S0022-3115(97)00015-9

The present study forms part of a larger program performed at the European Institute for Transuranium Elements to better understand the parameters and conditions of the formation of this rim structure, or high burnup structure. General aspects of the rim effect were dealt with in Ref. [2], the oxygen potential of the rim zone of the fuel employed in the present work was also measured and shown to be that of a stoichiometric oxide [4], and a detailed ion implantation study had shown that grain-subdivision, or polygonization, can also be produced in UO_2 by controlled ion bombardment with insoluble fission product ions (Xe, I) [5]. This latter work has also given some insight into the parameters of the formation of polygonization. It was extended by high resolution transmission electron microscopy, HRTEM, to study the formation of subgrain boundaries in more detail [6]. Other work performed in the hot cells of the institute [7] determined fuel porosity, volume pore density, pore size distribution and grain size distribution of the new subdivided grains in PWR fuel in the burnup range 40–67 GWd/tM.

The temperature and burnup conditions of the present fuel are dealt with in a companion paper [8]. Furthermore, modelling of burnup profiles is being done [9,10] and a tailor-made reactor irradiation has been started in joint work between CRIEPI, Tokyo, the OECD Halden project, Norway and ITU Karlsruhe [11] to determine the threshold burnup for polygonization as a function of fuel temperature. A recent summary of some of the above investigations is contained in Ref. [12].

2. The investigated fuel and specimen preparation for electron microscopy

The high burnup UO_2 investigated in the present study originated from a fuel rod irradiated in the Danish heavy water reactor at Risø. The fuel pellets had a diameter of 12 mm. The initial enrichment in U-235 was low (1.46%). However, the average burnup was high and amounted to 7.9% FIMA for the cross-section from which the fuel pieces for TEM examination were taken. The highest burnup in the rim region, as calculated by Kinoshita et al. using the codes ANRB and VIMBURN [13,14] and as determined from the local concentration of Nd [15] was about 2.8 times higher, i.e. in excess of 200 GWd/tM. More details of temperature and burnup calculations are communicated in a companion paper [8], explaining also nature and consequences of the high temperature period at about half the final burnup.

The major difficulty in making an electron microscopy analysis of the rim region in UO_2 fuel with presently used burnups (range 40–60 GWd/tM) is to ensure that the material examined comes exclusively from the first 200 μm depth of the pellet since this is the thickness of the restructured rim zone in such fuel. This effectively precludes specimen preparation by electropolishing, since it is not possible to control precisely the position of perforation, and consequently the area available for examination by TEM.

This problem was solved by preparing samples by taking very small pieces of fuel immediately adjacent to the cladding, extracted from a thin slice of the fuel cross-section. The best definition of the radial location was obtained when a fragment of fuel directly attached to the cladding could be recovered. These pieces were then crushed under methanol, and drops of the resulting suspension were allowed to dry on thin carbon films supported on copper grids. The small pieces of fuel left on the films were often thin enough for transmission electron microscopy. The samples were examined in a Hitachi H700 200 kV TEM which has been specially adapted for the analysis of radioactive samples, and is directly connected to a glovebox system [16,17]. This microscope is equipped with a secondary electron detector enabling very high resolution SEM images to be obtained, and with a Tracor Northern TN5500 energy dispersive X-ray analysis system. One advantage of this powder method of sample preparation is that the bulk of the specimen is small, thus minimizing the background radiation level and permitting qualitative energy dispersive X-ray analysis to be performed rather easily. In addition, the sample is not chemically affected by an electrolyte which might tend to dissolve out metallic fission product precipitates. The disadvantage of this method is that very precise radial-positional information is not available for the fragments of fuel examined either, though it is obvious that all pieces originate from the outermost 200 μm of the fuel.

In addition to the examination of a number of fuel pieces from the rim area with TEM, a sample from near to the fuel center was also examined by transmission electron microscopy for comparison purposes.

The investigation of the fuel structure was continued with a SEM examination of larger pieces of this fuel in the institute hot cells, extending the radial depth of the investigation to nearly 2 mm. These pieces were too active to have been examined in the above-mentioned Hitachi STEM. Therefore, the scanning electron microscope (Jeol 35C) mounted in the hot cells and controlled remotely was used for this part of the work. Pieces chosen for examination were those where the outer pellet surface could be clearly defined. A full cross-section of the pellet was also examined, but this had previously been mounted and polished for optical metallography and the microstructure could only be revealed within the pores.

3. Experimental results

3.1. TEM and high-resolution STEM investigation of fuel from the rim zone

Both by TEM and SEM, significant microstructural differences were found between the rim of the fuel and the

Fig. 1. Transmission electron micrograph showing the fine scale subgrain structure at the fuel rim. The inset diffraction pattern shows the spread in subgrain orientations to be very small ($< 5°$).

central regions. The rim sample showed the expected development of a subgrain microstructure with a typical grain size of 0.15 to 0.30 μm within the original coarse grain structure. It also showed a lower overall dislocation density within the grains and a much lower density of intragranular fission gas bubbles and precipitates than is normally found in the cold part of a fuel before grain subdivision occurs.

The electron diffraction pattern of grain-subdivided fuel pieces were those of UO_2. In addition, semi-quantitative analysis using energy dispersive X-ray analysis showed no detectable change in the chemical composition of the fuel

Fig. 2. Transmission electron micrograph showing the subgrain structure at the rim of the fuel, demonstrating the low density of dislocations found within the structure. A low density of precipitates is found, but fission gas bubbles are almost absent.

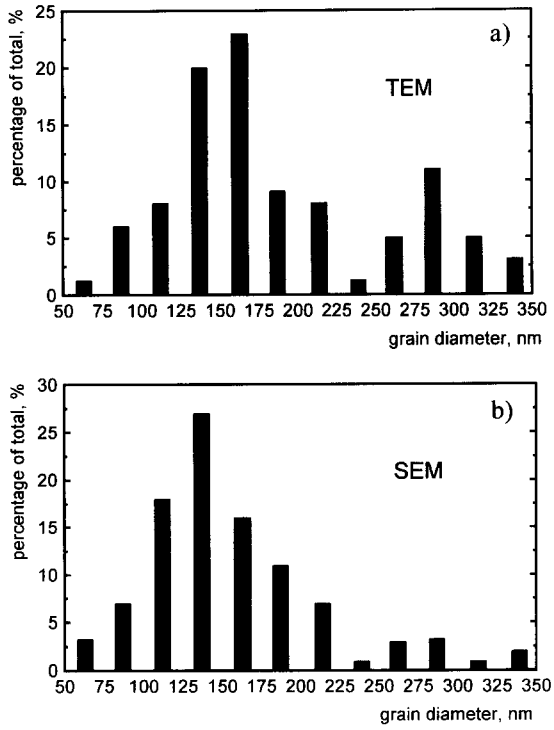

Fig. 3. Histogram of the measured subgrain sizes as revealed by TEM (a) and SEM (b).

at the rim, neither within the grains nor on the grain boundaries. A fully quantitative determination of fission products contained in the rim structure with the EDX technique is difficult since the sensitivity is reduced by the background activity of the samples, even if small pieces are examined.

3.1.1. The subgrain structure

This was the principal microstructural modification, and it could be observed directly by TEM, or by high resolution SEM on the fractured fuel surfaces and, particularly clearly, on the surfaces of exposed pores. Figs. 1 and 2 show examples of the typical rim microstructure as observed by transmission, with the diffraction pattern shown as inset. The total absence of any internal structure within the small grains of Fig. 1 should be noted. The misorientations between pairs of subgrains was found to be typically 2–7°. A histogram of the measured subgrain sizes as revealed by TEM is shown in Fig. 3a. The distribution appears to be bimodal with peaks at $\simeq 0.16$ and 0.30 μm.

Fig. 4 shows a corresponding SEM image of the fracture surface of a fuel fragment from the rim zone, where the subgrains are visible. The histogram of subgrain sizes determined from the SEM micrographs, taken on the same fuel pieces as used for TEM, but working in the scanning mode was similar to that based on TEM results (see Fig. 3b). These histograms are based on measurements of some

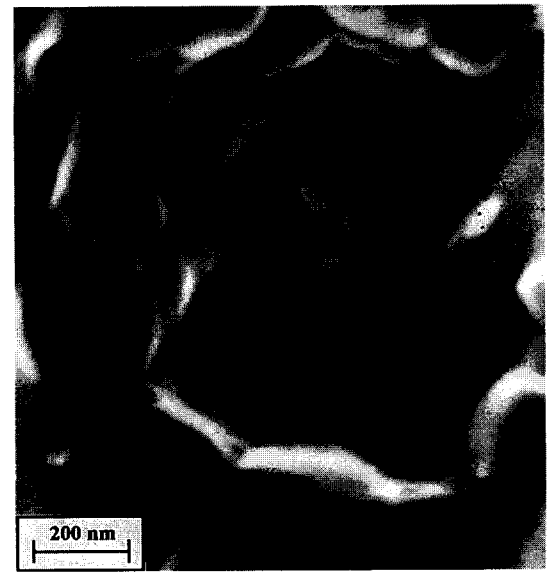

Fig. 4. Scanning electron micrograph of a fractured fuel surface at the rim, showing the subgrain structure corresponding to the TEM micrographs.

four hundred grains and represents the raw data on two-dimensional equivalent diameters, no correction having been applied to give a three-dimensional distribution.

The subgrain size histograms were approximately constant from one fuel fragment to another in this sample, but

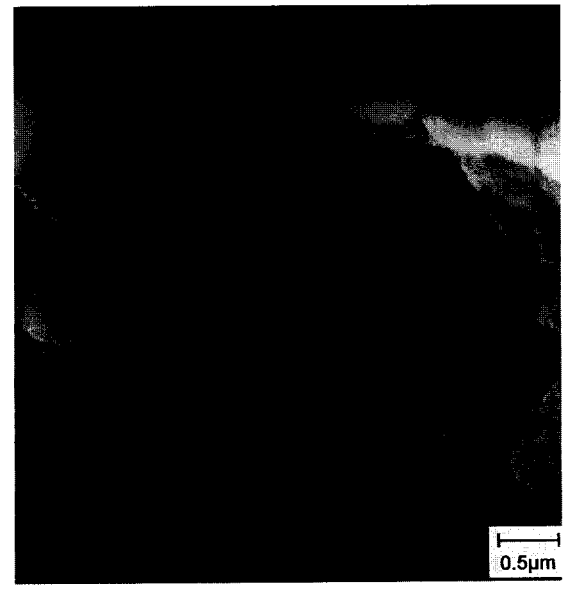

Fig. 5. Scanning electron micrograph showing the mottled surface and the possible 'two-tier'-type structure of the subgrains clustered into units about one tenth the size of the original grains of the as-fabricated fuel.

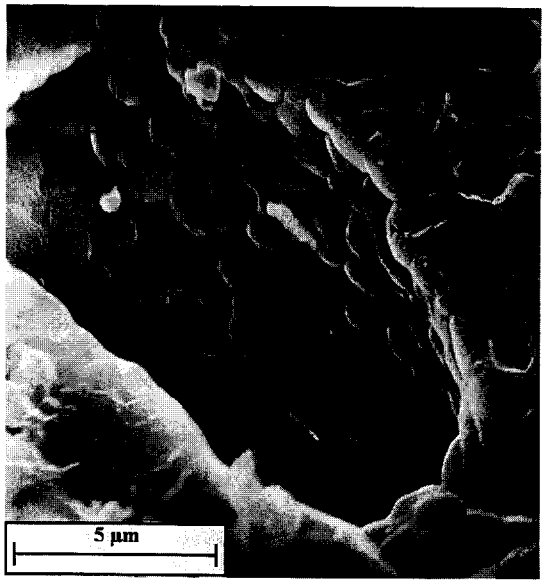

Fig. 6. Scanning electron micrograph of a fractured fuel surface showing how the sub-grain structure is particularly clearly visible on the inner surfaces of large pores.

differed from those measured on a full fuel cross-section, reported in Section 3.2, in that the peak is shifted in the latter case to a higher mean grain size of 0.32 μm, corresponding to the second peak of the bimodal histogram of Fig. 3a. The reason for this difference is not clear, but it is considered to be significant. The results obtained by TEM and STEM may arise because the material examined came from the very outermost rim of the pellet, but this can unfortunately not be checked because of the method which had to be used for the specimen preparation (see Section 2).

In some areas of these rim samples, another subgrain system could be identified in which the new grains had a mottled surface and gave the appearance of being clusters of much smaller subgrains. This class of new grains had an average size of 0.8 μm which is about one tenth of the average size of the original grains of the as-fabricated fuel. These larger grains (or units of grains) were separated by a high degree of porosity, and they were only found in bigger pores. An example of this type of structure is shown in Fig. 5. In Fig. 6, in a very large pore, possibly a pre-existing sintering pore, the structure is clearly seen, since in these very big pores the new grains are particularly big as well. This subgrain system was, however, only occasionally seen, always in connection with big pores. Most subgrains were small, as shown in Fig. 4.

3.1.2. The dislocation microstructures

Dislocation densities were measured in the TEM using the line intercept method [18,19], with care taken to allow for diffraction contrast effects which can lead to dislocation invisibility under certain combinations of dislocation Burgers' vector and diffraction conditions. The subgrains show a much lower dislocation and defect density than the central regions of the fuel. Some of the smaller subgrains appear to be almost defect free, checked under a wide range of diffracting conditions in the TEM. The average matrix dislocation density in the rim material averaged over all grains was measured to be approximately 5×10^9 cm cm^{-3}, but this was very inhomogeneously distributed,

Fig. 7. Transmission electron micrograph showing the typical microstructure of dislocations and dislocation loops at the fuel center.

Fig. 8. High magnification TEM micrograph showing subgrain boundaries without gas bubbles and with Moire fringe contrast.

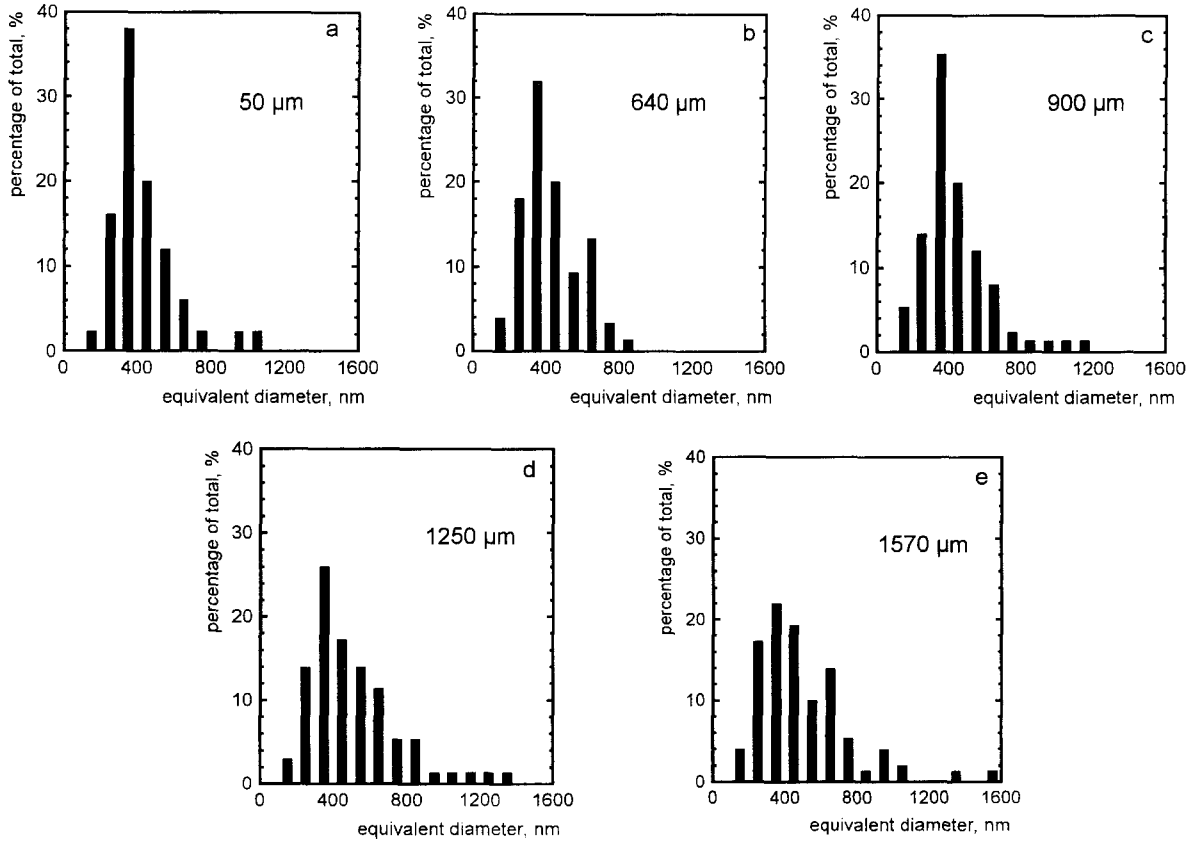

Fig. 9. Subgrain size histograms for various depths from the fuel surface.

compared with a homogeneous value of 2.5×10^{10} cm cm^{-3} in the central zones of the fuel.

The microstructure at the center also contained a high density, measured to be 5.5×10^{14} cm^{-3}, of large dislocation loops in the size range 12 to 50 nm. These loops were absent in the rim material. An example of the microstructure at the center is shown in Fig. 7.

3.1.3. Fission gas bubbles and precipitates

The rim samples showed no (or at the most very few) small intragranular fission gas bubbles in the size range < 10 nm in the subgrain structure, similarly no precipitates of the same size range. This can be demonstrated by the high magnification TEM micrograph in Fig. 8 in which typical subgrain boundaries are imaged showing Moire fringe contrast with a resolution of about 0.7 nm. Under steady-state irradiation conditions up to a burnup of around 40 GWd/tM, a high density of small fission gas bubble/precipitate pairs would be expected within the grains in the cold part of the fuel [20]. However, there was a low density of spherical metal precipitates with an average diameter of 35 nm on the grain boundaries.

At the fuel centre large five-metal particles up to 5 μm in diameter were found. In addition, a population of small fission gas bubbles linked to precipitates was present.

3.2. SEM investigation covering all of the fuel

As mentioned in Section 2, larger pieces of the above fuel, and also a full cross-section, were analyzed by SEM. The pieces selected were those where the outer pellet surface could be clearly recognized.

The typical 'rim' structure of very small subgrains could be found up to a depth of 1650 μm from the fuel surface, but the proportion of grains showing the effect decreased with depth. At 1700 μm the structure was no longer found at all, this thus can be taken to represent the limit for this particular fuel. Subgrain size histograms were constructed for various depths, based on up to 200 grain size measurements, and examples of these from 50 μm depth to 1570 μm are shown in Fig. 9a–e. Fig. 10 shows a typical example of the subgrain structure at a depth of 1200 μm.

It is interesting to note that the grain size histograms do not vary very significantly with depth into the fuel, and always show a peak between 0.3 and 0.4 μm. Very similar histograms were also recently reported by Spino et al. [7] for PWR fuels at burnups between 40 and 67 GWd/tM. The main variation with depth is the decreasing proportion of regions showing this structure as opposed to the normal grain structure of the fuel, from 100% at the very rim to a very small proportion at depths > 1 mm.

At a depth of 1.6 to 1.65 mm from the fuel surface, grain subdivision occurred only apparently at very few preferential sites, at grain boundaries or within pores.

4. Discussion

The present work was performed in 1992 and 1994 [27] in order to obtain statistically meaningful results on the microstructure of high burnup UO_2 following grain subdivision or polygonization to cause the formation of the 'cauliflower structure'. A fuel with a cross-section averaged burnup of 7.9% FIMA and with a period of high temperature at about half this burnup was selected for this action. This section reached a very high burnup at its surface, i.e. $\simeq$ 23% FIMA. The TEM specimens originated

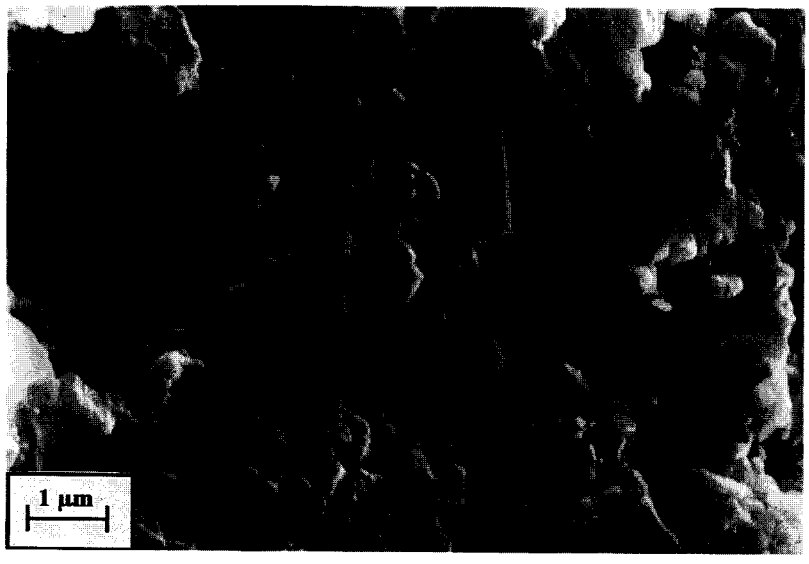

Fig. 10. Scanning electron micrograph of the typical subgrain structure found at a depth of 1200 μm from the fuel surface.

definitely from the first 200 μm, hence the zone with full development of the high burnup structure. With SEM, the (local) formation of this structure deeper in the pellet (up to about 1.65 mm) could also be observed. Also, extensive calculations on the irradiation history and on fuel temperatures have been made [8]. It is not the aim of this paper to provide an exact temperature/burnup relation and a final explanation of the polygonization process. Such actions are proceeding and will be reported later.

For the TEM specimens, an exact radial positioning within the above 200 μm and therefore an exact attribution of burnup to individual TEM specimens is not possible as it is for SEM analysis. The individual TEM pieces have therefore experienced polygonization at different times during the irradiation, i.e. they have experienced a further irradiation period of a duration varying from sample to sample, introducing new fission damage and new fission products following the polygonization process. In principle, one could anticipate that some of the TEM specimens studied here, or in similar work elsewhere, might have experienced two polygonization processes, though this is unlikely as explained in the companion paper [8].

Notwithstanding this fact, the extensive TEM data collected here are internally consistent in terms of size of subgrains, dislocation structure and appearance of fission gas bubbles and fission product precipitates. Also, the observed morphology is in good agreement with results from other laboratories [15,21–26]. It is no wonder, however, that small differences exist between these studies, e.g. in the degree of misalignment or the presence of small fission gas bubbles. Obviously, since the exact local burnup of a given TEM specimen from the fully polygonized outer rim with its steep burnup gradient is not known, it is very unlikely that any given sample has experienced grain subdivision just at the end of the irradiation. Also, all of the specimens of the present TEM and high resolution SEM work originated definitely from this proper rim zone. This is not necessarily the case for all of the other work. It was known before (e.g. [7,14]), and it is shown hereby that at extended burnup, polygonization can occur deeper in the UO_2 fuel, e.g. in the fuel of the present study up to a depth of 1.65 mm, though only to a very small proportion at depths > 1 mm and despite the fact, that at this depth of 1.65 mm, the fuel had experienced a calculated [8] local temperature of 1200°C and high gas release ($\simeq 70\%$) at about half its burnup. It is not a priori clear that the structure of such isolated areas of grain subdivision are identical with that of the proper polygonized rim zone. Therefore, caution should be taken when basing general conclusions for the (fully restructured) rim zone on observation on such isolated areas. The possible mistakes involved were definitely avoided in the present work.

The calculated temperature–time history of the outermost 200 μm of the fuel [8] shows that the local temperature was between 500 and 400°C up to a cross-section averaged burnup of 55 GWd/tM and that it decreased to about 380°C at the end of the irradiation. In contrast, the restructuring front ($\simeq 1.65$ mm depth) had experienced a long high temperature period of $\simeq 1200$°C local temperature between 4 and 5.2% FIMA local burnup with a subsequent further irradiation for 650 days at around 800°C to its final local burnup of 7.3% FIMA [8]. The detailed time histories of local burnup, local temperature and local fission rate and the implication for initiation and development of grain subdivision and polygonization in UO_2 during irradiation are given in a companion paper [8].

5. Summary

The TEM/SEM examination of material taken from the rim region (the first 200 μm from the pellet surface) of a high burnup UO_2 fuel with 74 GWd/tM cross-sectional burnup showed the microstructure to consist of low angle subgrains on a very fine scale (150 to 300 nm diameter). The development of this structure does not involve chemical reactions of the UO_2 matrix and thus results from physical processes alone. The misalignment between neighboring grains was small, hardly any fission gas bubbles were found and the dislocation density was also very low.

A SEM investigation showed that grain subdivision occurred to a depth of $\simeq 1.65$ mm. At this depth, the fuel had experienced a calculated local temperature of 1200°C for 280 days at about half the final burnup causing gas release and damage recovery. The fraction of the fuel affected by grain subdivision decreased from 100% at the surface to small values at depths > 1 mm. The size of the new grains was largely independent of the depth in the zone of $\simeq 0.2$ to 1.65 mm with a peak in the histograms between 0.3 and 0.4 μm. These results and their possible implications to increase the understanding of the mechanism causing grain subdivision are further discussed in a companion paper [8].

Acknowledgements

The authors would like to thank the staff of the hot cells of ITU (M. Coquerelle and his team) for their help in preparing the specimens for the SEM/TEM investigation, and J. Spino for fruitful discussions.

References

[1] Hj. Matzke, H. Blank, M. Coquerelle, K. Lassmann, I.L.F. Ray, C. Ronchi, C.T. Walker, J. Nucl. Mater. 166 (1989) 165.
[2] Hj. Matzke, J. Nucl. Mater. 189 (1992) 141.
[3] Hj. Matzke, J. Spino, Proc. IEQES 96, J. Nucl. Mater., in press.

[4] Hj. Matzke, J. Nucl. Mater. 208 (1994) 18.
[5] Hj. Matzke, A. Turos, G. Linker, Nucl. Instrum. Methods B91 (1994) 294.
[6] Hj. Matzke, L.M. Wang, J. Nucl. Mater. 231 (1996) 155.
[7] J. Spino, K. Vennix, M. Coquerelle, J. Nucl. Mater. 231 (1996) 179.
[8] M. Kinoshita, T. Kameyama, S. Kitajima, Hj. Matzke, J. Nucl. Mater., submitted.
[9] K. Lassmann, C. O'Carroll, J. van de Laar, C.T. Walker, J. Nucl. Mater. 208 (1994) 223.
[10] K. Lassmann, C.T. Walker, J. van de Laar and F. Lindström, J. Nucl. Mater. 226 (1995) 1.
[11] M. Kinoshita, T. Matsumura, T. Kameyama, S. Kitajima, E. Kolstad, Hj. Matzke, presented at the Extended Halden Project Group Meeting, Bolkesjø, Oct. 31–Nov. 4, 1994.
[12] H. Matzke, in: Proc. 8th World Conf. on Ceramics, CIMTEC, Florence, June 29–July 4, 1994, Ceramics Charting the Future, ed. P. Vincenzini (Techna Srl., 1995) p. 2913.
[13] T. Matsumura, T. Kameyama, IAEA Technical Meeting on Water Reactor Fuel Element Computer Modelling in Steady-State, Transient and Accident Conditions, Preston, UK, 1988, pap. 1.6.
[14] T. Kameyama, T. Matsumura, M. Kinoshita, Proc. Int. Topical Meeting on LWR Fuel Performance, Fuel for the 90's, Avignon, France, 1991, Vol. II, ANS/ENS, 1991, p. 620; CRIEPI-Report T 89024, Tokyo, 1990.
[15] C.T. Walker, T. Kameyama, S. Kitajima, M. Kinoshita, J. Nucl. Mater. 188 (1992) 73.
[16] I.L.F. Ray, H. Thiele, H. Blank, J. Phys. (Paris) 45 (C2-849) (1984) 1.
[17] I.L.F. Ray, H. Thiele, Proc. Hot Cell Workshop, Karlsruhe, 1981.
[18] R.K. Ham, Philos. Mag. 6 (1961) 1183.
[19] P.B. Hirsch, J.W. Steeds, N.P.L. Symposium No. 15 (HMSO, 1964).
[20] I.L.F. Ray, H. Thiele, Hj. Matzke, in: Fundamental Aspects of Inert Gases in Solids, eds. S.E. Donnelly and J.H. Evans (Plenum, New York, 1991) p. 457.
[21] Hj. Matzke, G. Schumacher, eds., Nuclear Materials for Fission Reactors, J. Nucl. Mater. 188 (1992) 348 pp, special issue.
[22] I.L.F. Ray, H. Thiele, Hj. Matzke, J. Nucl. Mater. 188 (1992) 90.
[23] L. Thomas, C.E. Beyer, L.A. Charlot, J. Nucl. Mater. 188 (1992) 80.
[24] K. Une, I. Nogita, S. Kashibe, M. Imamura, J. Nucl. Mater. 188 (1992) 65.
[25] M.E. Cunningham, M.D. Freshley, D.D. Lanning, J. Nucl. Mater. 188 (1992) 19.
[26] K. Nogita, K. Une, Nucl. Instrum. Methods B91 (1994) 301.
[27] I.L.F. Ray, H. Matzke, H. Thiele, M. Kinoshita, in: Reports European Commission, Annual Reports 1992 and 1994, Institute for Transuranium Elements, EUR 15154 EN, 1933, p. 17, EUR 16152 EN, 1995, p. 21.